

# Evaluation Model of DC Current Distribution in AC Power Systems Caused by Stray Current of DC Metro Systems

Aimin Wang, Sheng Lin, *Member, IEEE*, Ziheng Hu, Junyi Li, Feng Wang, Guoxing Wu, and Zhengyou He, *Senior Member, IEEE*

**Abstract**—With the rapid development of the DC metro system, the stray current may bring new challenges to the AC power system. Especially, the stray current of the DC metro system flowing in the AC power system may cause many serious consequences such as the corrosion of the grounding grids, plenty of harmonics, and the dc bias of transformers. Therefore, it is significant to evaluate the dc current distribution in the AC power system caused by the stray current. In order to evaluate the dc current distribution, a coupled simulation model both considering the DC metro system and the AC power system is proposed in this paper. Moreover, the earth and the grounding system are both used as the coupling elements in the proposed model. The correctness of the proposed model is verified by the comparison of the calculation results and the field test data. Furthermore, based the proposed model, the dc current distribution in the AC power system is evaluated and analyzed. The results indicate that the dc current distribution is affected by the trains operating conditions and the relative position between the DC metro system and the AC power system.

**Index Terms**—DC metro system, stray current, AC power system, coupled simulation model, dc current distribution.

## I. INTRODUCTION

### A. Background

IN the AC power system, the coupled dc current may cause a lot of serious problems, such as corrosion of the grounding grid, protection mistake, and plenty of harmonics [1]. In addition, with the dc current increasing, the transformers in the AC power system may be under dc bias if their neutral points are grounded. The dc bias can cause acute vibration, great noise, and high temperature of the transformer, even make the transformer fail [2]. Thus, the dc current in the AC power system brings many troubles and threatens the safety of the system.

At present, many authors have investigated the dc current distribution in the AC power system [3]–[5]. Since the dc current is mainly caused by geomagnetism and high voltage direct current (HVDC), few papers paid attention to the dc current distribution in AC power system caused by the stray

current of the DC metro system. However, leakage currents from DC metros injected into AC power system have resulted in the dc bias of transformers, such as Guangzhou, Shenzhen, and Guiyang in China. Moreover, with the DC metro system gradually becoming networked and highly dense [6]–[10], the increasing stray currents may bring new challenges to the AC power system. Therefore, it is important to evaluate and analyze the dc current distribution in AC power system caused by the stray current of DC metro system.

### B. Literature Review and Motivation

In HVDC systems, the positions of the grounding electrodes are fixed, and the leakage dc currents of the grounding electrodes inject in the AC power system mainly through the earth [11]. Thus, when modeling the grounding electrode of the HVDC, the grounding electrode is always equivalent to a constant dc current source and the direction of the dc current is only flowing into the earth [12]. In AC power system, the dc current travels through the connected electrical devices. Thus, based on the dc current flowing path, the devices are equivalent to dc resistance conductors [1]. And the equivalent conductors are connected together based on the structure of the AC power system, which constitute a dc current circuit [13]. Through the complex circuit-field calculations or simulations of the grounding electrode and AC power system, dc current distribution in the AC power system is obtained [14], [15].

However, different from the HVDC grounding electrode with the constant position, the stray current of the DC metro system is varied with the trains operations, grounding schemes and parameters of rails [16]–[18]. The magnitude, position and flowing direction of the stray current are unpredictable and stochastic in time and space. Therefore, the stray currents of the DC metro system cannot be equivalent to a constant dc current source with a fixed position and flowing direction. It is crucial to establish the stray current simulation model and calculate the stray current according to the geographical distribution of the DC metro system.

In addition, different from the HVDC that the dc current flows into the AC power system through the earth, the stray current of DC metro system flows into the AC power system through not only the earth but also the grounding systems. The grounding systems of the DC metro system and the AC power system are shown in Fig. 1.

In the DC metro system, the flat steel of the third rail, the flat steel of the cable holder and the metal shielding layer of

This work was supported by the National Natural Science Foundation of China under grant 51677153.

A. Wang, S. Lin, J. Li, F. Wang, and Z. He are with the School of Electrical Engineering, Southwest Jiaotong University, Chengdu 610031, China (email: wam501382@163.com, slin@swjtu.edu.cn, lji.2018@foxmail.com, wangfeng\_1304@163.com, hezy@swjtu.edu.cn).

Z. Hu, and G. Wu are with the Shenzhen power supply bureau co. LTD, China Southern Power Grid, Shenzhen 518000, China (email: huziheng@sz.csg.cn, wuguoxing@sz.csg.cn).

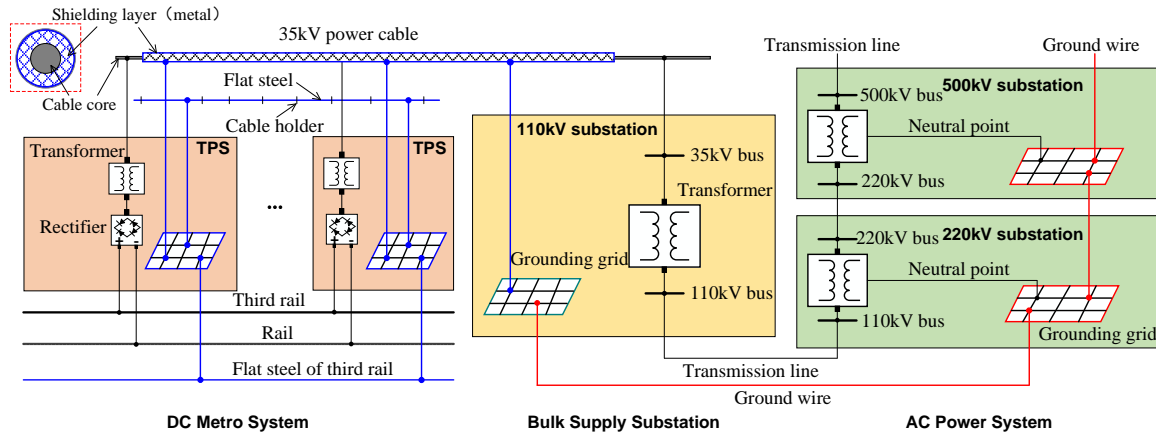


Fig. 1. Grounding systems of the DC metro system and AC power system.

the cable are all grounded and connected to the grounding grids in traction power substations (TPSs) [19], [20]. Thus all the grounding grids of the TPSs are connected together. In DC metro system, the TPSs are supplied by the bulk supply substations through 35kV power cables. And the shielding layers of 35 kV power cables are grounded to the grounding grids of the bulk supply substations and TPSs. Therefore, the grounding system of the DC metro system is an integrated grounding system.

Meanwhile, the bulk supply substations are powered by the 220 kV and 500 kV substations. And the ground wires are grounded to the ground grids of the bulk supply substations and the 220kV and 500kV substations [21]. Thus, the grounding system of the AC power system is also an integrated grounding system. Through the grounding grids of the bulk supply substations, the grounding system of the DC metro system is connected to the grounding system of the AC power system.

Therefore, when the dc current leaks from the rails into soil, firstly the dc current can flow into the grounding system of the DC metro system. Then, through the grounding system, the dc current can flow into the grounding grids substations in AC power system. Finally, through the transformers neutral points, the dc current flows into transformers in AC power system. Therefore, evaluating the dc current distribution in the power system caused by DC metro system, not only the earth but also the grounding systems are very important.

### C. Contribution of This Paper

In order to solve the aforementioned problem, this paper proposes a coupled simulation model to evaluate the dc current distribution in AC power system caused by the stray current of DC metro system. In the proposed model, the DC metro system and the AC power system are both considered. Moreover, according to the coupling relationship between the DC metro system and the AC power system, the earth and the grounding system are both used as the coupling elements. The correctness of the proposed model is verified through the comparison of the simulation results and the field test data of the neutral point dc current of the transformer near the Shenzhen DC metro line. Based on the coupled simulation

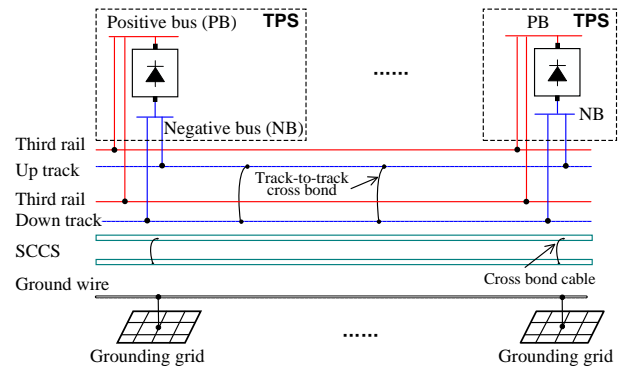


Fig. 2. Schematic representation of the DC metro system.

model and the operation conditions of trains, the dc current distribution in AC power system is obtained. With the train operation time, the direction of the neutral point dc current is changed with positive-negative alternating transformation, and the period time of the change approximately generally equals to the headway of the trains. According to the position distribution of the transformers, the neutral point dc currents of the transformers near the DC metro line especially the depot are larger than that of substations in the far away.

The remainder of this paper is organized as follows. The modeling principle of the proposed coupled simulation model is presented in Section II. Section III presents the coupled simulation model and verifies the correctness of the presented model. The results of the evaluation and analyse of the dc current distribution are presented in Section IV. V concludes the whole paper.

## II. MODELLING PRINCIPLE

The proposed coupled simulation model is established in MALZ module of the CDEGS software [22]. In the proposed model, the electrical elements of the DC metro system and AC power system are equivalent to conductors with the same dc resistance parameters. And, since conductors in MALZ are required to be placed under the ground [6], [15], the equivalent are modelled with an outer perfect insulation layer to represent the exposure to air.

In the proposed model, the stray current distribution and the structure of the AC power system are crucial for evaluating

the dc current distribution in the AC power system. As the dc current sources, the stray current distribution determines where the dc current leaks into the AC power system. Thus, in order to obtain the stray current distribution precisely, the modeling of the DC metro system is essential. The structure of the AC power system determines the coupling path of the injected dc current. Thus, to obtain the dc current distribution in AC power system accurately, the model of the AC power system is important.

Moreover, the grounding systems of the DC metro system and the AC power system are connected and have the through-type structure as shown in Fig. 1. Therefore, in the proposed model, the earth and the grounding system are both used as the coupling element. According to the structure of the proposed model, the model can be divided into two parts: the model of the DC metro system and the model of the AC power system.

#### A. Model of the DC Metro System

In the model of the DC metro system, the electrical elements should be considered, including the third rails, TPSs, up and down tracks, the stray current collector system (SCCS), the grounding system, and the soil. Referencing the structures as shown in Fig. 2, the model will be described in detail:

1) *Third Rail*: In the DC metro system, the third rail is used to transmit dc current for the train. On each track, the radius of the third rail is 3705 mm<sup>2</sup> and the resistivity is 0.008 Ω/km. Referencing the parameters and the number of the third rail, the third rails of the two tracks are equivalent to two longitudinal conductors in the coupled simulation model as shown in Fig. 3. The resistance of the equivalent conductor is 0.008 Ω/km with the radii of 0.034 m. Moreover, the equivalent conductors are modelled with a perfect insulating outer layer and then placed in the concrete.

2) *TPS*: In the DC metro system, the traction currents flow out of the TPSs to the third rails, and return currents flow to the TPSs through the rails. Therefore, the TPSs can be equivalent to the conductor connecting the rails to the third rails as shown in Fig. 3. Moreover, the third rails of the up and down tracks are connected by the positive bus of the TPS. Therefore, the TPS also should be equivalent to the conductor connecting the third rails of the up and down tracks. Referring the equivalent dc resistance of the TPS [23], the resistance of the equivalent conductor is 0.054 Ω, and the conductors are modelled with an outer insulating layer.

3) *Track*: In the track of the DC metro system, two rails are running for supporting trains and returning dc current. As shown in Fig. 2, the two running rails (e.g., GB60kg/m) can be equivalent to one conductor having a half resistance and twice cross-section than the rail. Considering the wear and corrosion during the trains operation [6], the resistance of the equivalent conductor is 0.02 Ω/km and the radius is 0.069 m. The insulator pads and fasteners of the rails are the main factors forming the rail-to-earth conductance. Thus, the insulator pads and fasteners can be equivalent to a resistive coating of the conductors. According to the rail-to-earth resistance [24], the resistive coating of the conductor is set to 40 Ω·km [6] which is benchmarked against the permitted minimum value posed by

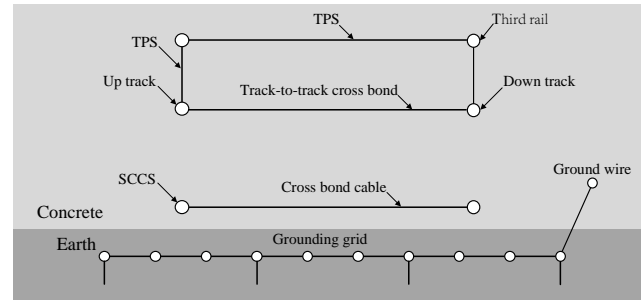


Fig. 3. Plan view of the stray current simulation model.

EN 50122-2 and IEC 62128-2 [25], [26]. To balance the return current and mitigate the stray current of two tracks, the track-to-track cross bonds are installed in the connecting bypasses [19]. According to the positions of the connecting bypasses in the project, the track-to-track cross bond is equivalent to the conductor with the cross-section of 300 mm<sup>2</sup>, the resistance of 0.1905 mΩ [23].

4) *SCCS*: In the DC metro system, the SCCS is installed under the rails to collect the stray current. The SCCS is consisted of a set of longitudinal steel bars with resistance of 0.55 Ω/km and parallel structure [7]. Moreover, the SCCS of each track is connected by the cross bonding cables with the cross-section of 300 mm<sup>2</sup> at the train stations [23]. Therefore, in the coupled simulation model, the longitudinal steel bars of the SCCS can be equivalent to a longitudinal conductor as shown in Fig. 3. The cross bonding cables are equivalent to the transversal conductors bonded the two longitudinal equivalent conductors of SCCS under up and down tracks as shown in Fig. 3. The total surface area of the longitudinal equivalent conductor is equal to that of the longitudinal steel bars. The resistance of the longitudinal conductor is 0.1 Ω/km. And the resistance of the transversal conductor is 1.53 mΩ [23] with the cross-section of 300 mm<sup>2</sup>.

5) *Grounding System*: In the DC metro system, the grounding system includes the grounding grids and ground wire. The grounding grid is installed in the TPS with longitudinal and transversal steel bars. Referring the practical project, the grounding grid is 140 m × 40 m, and the resistance of the steel bar is 2 Ω/km. Therefore, in the coupled simulation model, the ground grid is equivalent to a 140 m × 40 m conductive grid of which the resistances of the equivalent conductors are 2 Ω/km with the radii of 7 mm. In the DC metro system, the ground wire is used to ensure the safety of the equipment including the flat steels of the cable holder and the third rail, and the cable shielding layer as shown in Fig. 1. Thus, in the coupled simulation model, the ground wire is equivalent to the conductor with the resistances of 0.1 Ω/km and the radii of 18 mm.

6) *Soil*: In the DC metro system, the soil includes two layers, the concrete and the earth. Thus, in the coupled simulation model, the soil can be modeled with two layers. The upper soil layer of the soil model is equivalent to the concrete and assigned a resistivity of 180 Ω·m. Moreover, the third rail, TPSs, two tracks, the SCCS, and the ground wire are modeled in the upper soil layer. The lower layer of the soil model is equivalent to the earth and assumed to have a

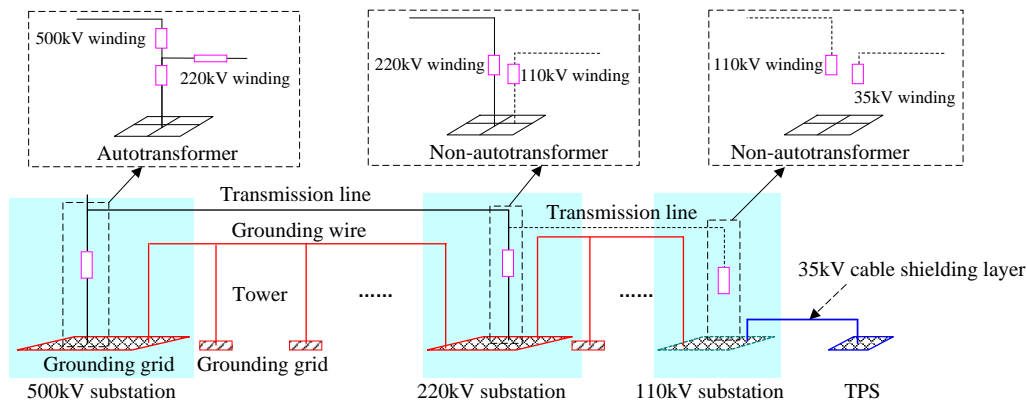


Fig. 4. simulation model of the AC power system.

resistivity of  $100 \Omega \cdot \text{m}$  [27]. Moreover, the grounding grids of TPSs are modeled in the lower soil layer.

### B. Model of the AC power system

In AC power system, the dc current is mainly affected by the dc resistances of the devices in the AC power system [1]–[4]. Therefore, in the coupled simulation model, the electrical elements of the ac power system are equivalent to conductors just with dc resistances. Moreover, because the conductors can not be modeled to expose to the air in MALZ, the equivalent conductors of the AC power system except the grounding grid are all set a completely insulated coating and placed in the soil. Referring the model of the AC power system as shown in Fig. 4, the equivalent conductors are described in more detail:

1) *Ground Grid*: In the AC power system, the grounding grids are installed in the substations and under the towers to protect the devices. In the substation, according to the code for design of the substation earthing [20], the resistance of the grounding grid is less than  $0.5 \Omega$ . Thus, according to the areas of the substations, the grounding grid of the 500kV substation is equivalent to a  $400 \times 400 \text{ m}^2$  conductive grid with conductor space of 25m. And the grounding grid of the 220kV substation is equivalent to a  $300 \times 300 \text{ m}^2$  grid with conductor space of 25m. In the AC power system, the resistance of the grounding grid of the tower is less than  $30 \Omega$ . Thus, the grounding grid of the tower is equivalent to a  $20 \text{ m} \times 20 \text{ m}$  conductive grid with conductor space of 10m. In the proposed model, the dc resistances of the conductors of the grounding grids are all set  $2 \Omega/\text{km}$  with the radii of 7mm.

2) *Transformer*: The windings of the grounded transformers of the substations are the paths through which the dc current flows into the AC power system easily. According to the winding structures of transformers, transformers can be divided into the autotransformer and the non-autotransformer [12], [28]. In 500kV substation, the transformer is usually the autotransformer of which the dc resistance of the 500 kV winding is about  $0.238 \Omega$  per phase, and the 220 kV winding is  $0.097 \Omega$  per phase [3]. In 220kV substation, the transformer is usually the non-autotransformer of which the dc resistance is less than  $0.6 \Omega$  [28]. Thus, the different windings of the grounded transformers in the substation are equivalent to the conductors with different structures as shown in Fig. 4. The

dc resistance of the equivalent conductor  $R_T$  is calculated by:

$$R_T = \frac{R_P}{3N_T} \quad (1)$$

where  $R_P$  is the dc resistance of the per phase winding of the transformer;  $N_T$  is the number of the transformers in the substation. It should be noted that the ungrounded non-autotransformer can be ignored when modeling the model because the dc current cannot flow through the windings [3]. While, since the DC current can flow through the ungrounded autotransformer, the ungrounded autotransformer should be modeled with the high voltage winding connecting to the low voltage winding [13], [29].

3) *Transmission Line*: In the AC power system, through the transmission line between the grounded transformers, the dc current can flow among the different substations. In the proposed coupled simulation model, the transmission line is equivalent to a conductor which connects to the windings of transformers as shown in Fig. 4. the dc resistance of the equivalent conductor  $R_L$  can be given by:

$$R_L = \frac{\rho_l L_l}{3S_l C N} \quad (2)$$

where  $\rho_l$  is the dc resistivity for the transmission line;  $L_l$  is the length of the transmission line;  $S_l$  is the sectional area of the single transmission line;  $C$  is the split number of per phase;  $N$  is the circuit number of the power transmission. It should be noted that transmission line connected to the ungrounded transformer can not be modeled because the dc current can not be spread through the ungrounded transformer [4].

4) *Tower*: In the AC power system, the transmission line is supported by towers. Towers are constructed with a steel structure and grounded through the ground grid. Therefore, in the coupled simulation model, the tower can be equivalent to the conductor with the dc resistance of  $2 \Omega/\text{km}$  as the same as the steel bar. Moreover, the equivalent conductor is connected to the grounding grid under the tower and insulated from the transmission line.

5) *Ground Wire*: In the AC power system, the ground wire is set up along the transmission line and supported by towers to provide prevention from lightning. In the substations, the ground wire is connected to the grounding grid. Along the transmission line, the ground wire is connected to the towers. Therefore, in the coupled simulation model, the ground wire is



equivalent to the conductor connected to the grounding grids of the substations and the towers along the transmission line. The dc resistance of equivalent conductor of the ground wire  $R_W$  is calculated by:

$$R_W = \frac{\rho_w L_w}{S_w N} \quad (3)$$

where  $\rho_w$  is the dc resistivity for the ground wire;  $L_w$  is the length of the ground wire;  $S_w$  is the sectional area of the grounding wire;  $N$  is the circuit number of the transmission lines.

6) *Cable Shielding Layer*: In 110 kV substation supplying for DC metro system, the shielding layer of the 35kV power cable is connected to the grounding grid. Meanwhile, in the DC metro system, the shielding layer of the 35kV power cable is also connected to the grounding grids of all the TPSs. According to the project, the dc resistance of the shielding layer of the 35kV cable per phase is generally about 2  $\Omega$ /km. Thus, in the coupled simulation model, the shielding layer of the 35 kV power cable can be equivalent to the conductor connected to the grounding grids of the TPSs and the 110 kV substation. If the 35 kV power cables are three phases and double-circuit lines, the dc resistance of the equivalent conductor is 0.34 $\Omega$ /km.

7) *Soil*: Since the DC metro system and the AC power system are coupled with the soil, the soil of the DC metro system is that of the AC power system. Moreover, in AC power system, some conductors are modeled with the outer perfect insulation layers, so the conductors can be put in any layers of the soil. In the coupled simulation model, the equivalent conductors of the AC power system are set in the lower layer of the soil.

Based on the modeling processes, the coupled simulation model can be established, in which the models of the DC metro system and the AC power system are coupled through the earth and the grounding system.

### III. MODEL VALIDATION

#### A. Description of the Coupled Simulation Model

Using the proposed modeling principle, the coupled simulation model of the Shenzhen metro line and the AC power system in the nearby vicinity is modeled as shown in Fig. 5. The geographical distributions and the structures of coupled simulation model are consistent with the practical project.

In the DC metro system, there are three parts including the mainline, the depot, and the parking lot as shown in Fig. 5. The mainline is used to support trains and transport passengers. While the depot and parking lot are used to park and maintain trains without SCCS. In the Shenzhen metro line, the distance of the mainline is 41.6 km. There are 30 stations along the DC metro line, among which there are 14 stations #1 to #14 with the TPS. The depot and the parking lot shown in Fig.5 are close to TPS #3 and #9 respectively and connected to the mainline through the tracks. The grounding system as shown the green line is distributed along the tracks of the mainline, depot, and parking lot. Moreover, in the depot and parking lot, there are no SCCS under the rails and the rails are grounded through the grounding grids.

TABLE I  
MINIMUM DISTANCE OF THE SUBSTATIONS FROM DC METRO LINE

Substation	A	B	C	D	E	F	G
Distance(km)	0.65	0.45	6.14	0.25	2.43	0.84	0.85

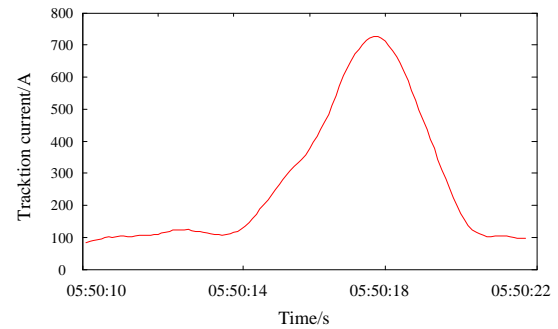


Fig. 6. Traction current of the first train.

In the AC power system, there are ten substations of which the grounding grids are connected by ground wires, the blue lines, as shown in Fig. 5. Based on the modeling principle, the neutral ungrounded transformers are ignored in the substations. Thus, according to the practice project, there are just six substations with neutral ungrounded transformers. Moreover, the neutral grounded transformers are connected by the transmission lines, as shown the red lines. The substations H, I, and J, as the bulk supply substations are respectively connected to the grounding system of the DC metro system through the shielding layer of the 35kV power cable, the black line, as shown in Fig. 5.

Moreover, the grounding grid of the 110 kV substations are connected to the grounding system of the DC metro system through the shielding layer of the 35kV power cable.

In the coupled simulation model, the minimum distances from the substations to DC metro line are shown in Table I. And the basic parameters of the coupled simulation model are shown in Table II.

#### B. Operational Condition

When the trains operating on the Shenzhen metro line, the operation conditions and positions of trains are complex and variable during the whole day. Under the complex operation conditions of trains, it is hard to understand where the neutral point dc current comes from. Thus, to validate the simulation model, a single event operation condition is required in which the simulation data can be compared with measurement data is preferred. Fortunately, there is a special operation period during the first train departing from the depot. During this period, there is no train on the mainline. Moreover, because the transformer in substation A is very near to the depot, the neutral point dc current will mainly be affected by the stray current caused by the first train. Therefore, to verify the validity of the coupled simulation model, the operation condition of the first train during the departure period is simulated.

During the first train departing from the depot, the first train is departing from the depot from 05:50:14 to 05:50:20

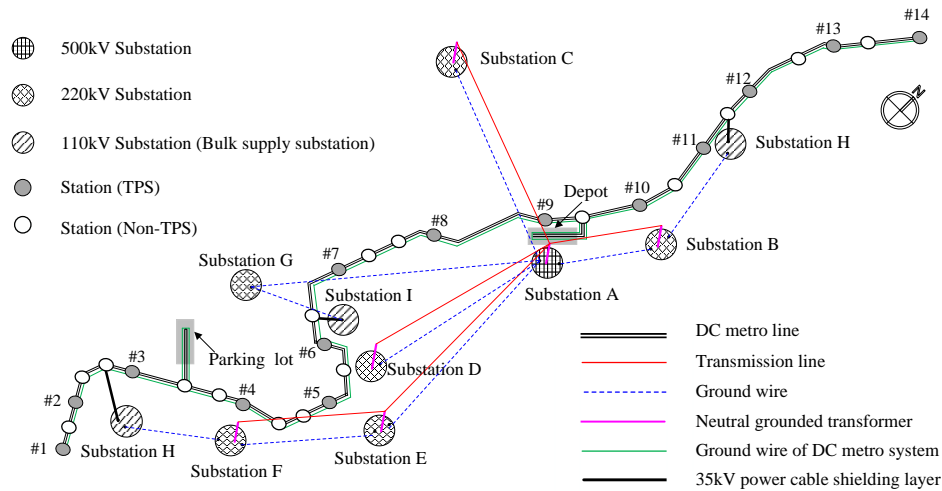


Fig. 5. Coupled simulation model of the DC metro line and AC power system in the nearby vicinity.

TABLE II  
MAIN PARAMETERS OF THE COUPLED SIMULATION MODEL

Model	Structure	Value
DC metro line	Track	0.02 $\Omega/\text{km}$
	SCCS	0.1 $\Omega/\text{km}$
	Ground grid	2 $\Omega/\text{km}$
	Ground wire	0.1 $\Omega/\text{km}$
	third rail	0.008 $\Omega/\text{km}$
AC power system	Ground grid	2 $\Omega/\text{km}$
	Ground wire	0.5 $\Omega/\text{km}$
	500kV transformer	1 $\Omega/\text{km}$
	220kV transformer	2 $\Omega/\text{km}$
	220kV Transmission line	0.01 $\Omega/\text{km}$
	Cable shielding layer	0.34 $\Omega/\text{km}$
Soil model	Concrete	180 $\Omega\cdot\text{m}$
	Earth	100 $\Omega\cdot\text{m}$

on May 11, 2019, and the first train is operating on the metro line linking the depot to the mainline supplied by the TPSs of the mainline. The traction current from 05:50:10 to 05:50:22 is shown in Fig. 6. The traction current of the train starts markedly increasing at 05:50:14, reaches the maximum 730 A about 05:50:18 and starts going down to 100A finally which may power the services facilities, such as the lights and broadcasts.

### C. Verification of the Coupled Simulation Model

Based on the coupled simulation model and the traction condition of the first train during the departure period from 05:50:10 to 05:50:22, the neutral point dc current of the transformer in substation A is calculated. Moreover, the neutral point dc current of the substation A is also tested during the departure period on May 11, 2019. The field test data and the calculation result are shown in Fig. 7. In the curves of Fig. 7, positive values indicate the dc currents flow into the transformer and vice versa.

Comparing the field test data and the calculation result of the neutral point dc current of the substation A, obviously, the two curves are very consistent from 05:50:14 to 05:50:20. When

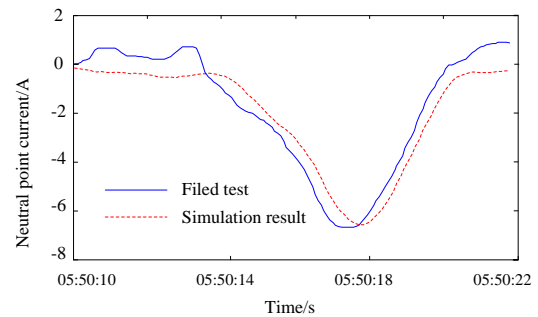


Fig. 7. The neutral point dc current of the transformers in substation A.

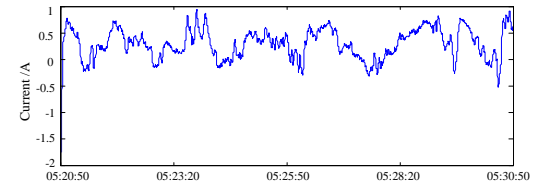


Fig. 8. The field test data of neutral dc current in substation A without stray current.

the traction current increasing, the neutral point dc current also increases. And during the traction condition of the train, the direction of the two neutral point dc currents are very consistent. During this moment, the curves are both negative that means the stray current flows into the transformer in substation A. That is, when the train tracking in the depot, the stray currents leak from the rails and flow into the substation A. Moreover, the higher the traction current is, the higher the neutral point dc current is. The maximum number of the calculation result is 6.7 A, which is similar to the maximum number of the filed test 6.8 A. And the time difference between the maximum numbers of the calculation result and field test is less than 1 s.

There are some differences between the calculation result and the filed test data when the train operating without traction. The difference error may be caused by the accuracies of the sensors and the monitor and the noise of the system. During 05:20:50 to 05:30:50, there is no train operating on the mainline and depot. The field test data of neutral dc current

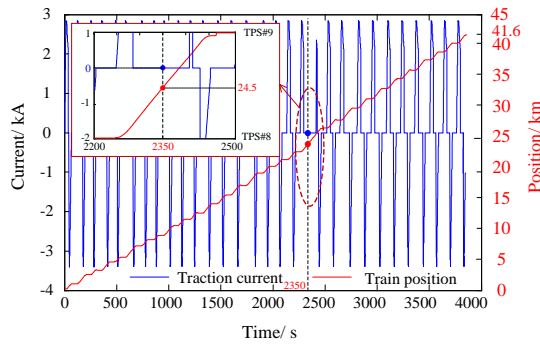


Fig. 9. The traction current and the position of the single train.

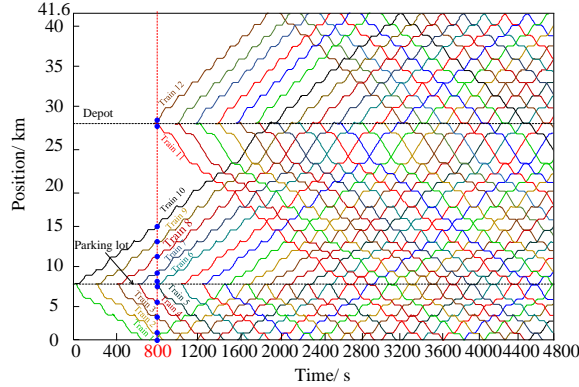


Fig. 10. Timetable of the trains on the Shenzhen metro line.

in the substation A is shown in Fig. 8. The field test data is not 0. The max number of the error is 0.88 A, and the min number is -0.5 A. It indicates that there is different error in the test data caused by the accuracies and noise of the sensors and the monitor.

However, the substation A is the closest to the first train, and the difference of the two curves is far less than the maximum number of the dc current in AC power system, so the coupled simulation model can be verified by the comparison result of the first train during the departure period. That is, the proposed coupled simulation model can be used to calculate and analyze the distribution characteristics of the dc current in the AC power system.

#### IV. EVALUATION AND ANALYSIS OF DC CURRENT DISTRIBUTION

According the field test data and the calculation results in the previous section, it shows the neutral point dc current can change with the train operation. Therefore, to evaluate and analysis the dc current distribution in the AC power system, the trains operation conditions including the trains positions and traction currents should be considered.

##### A. Operation Conditions of Trains

Based on the proposed coupled simulation model of the Shenzhen metro line and the AC power system in the nearby vicinity, when the train is operating in the mainline from #1 to #14 as shown in Fig. 5, the traction current and position of the trains are shown in Fig. 9. The red line is the traction current, and the blue line is the train positions which are calculated

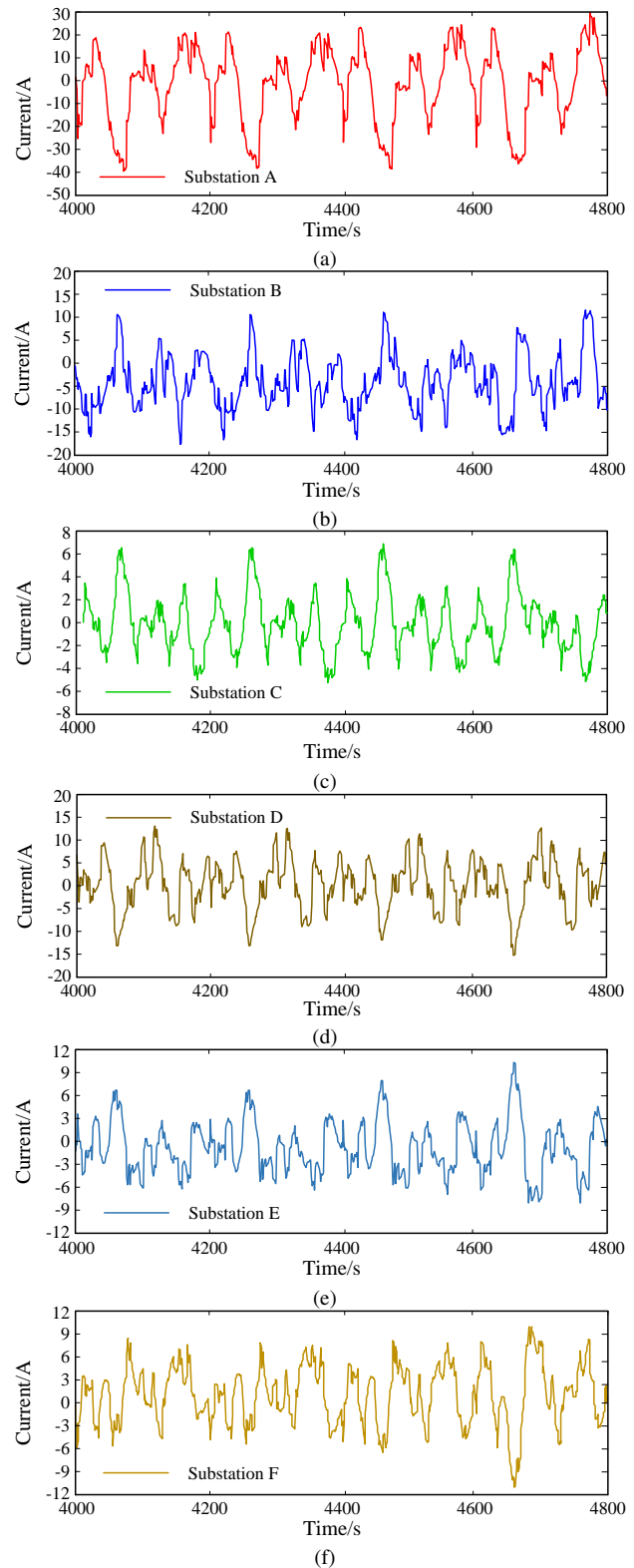


Fig. 11. The calculation results of the neutral point dc current. (a) The transformers in substation A. (b) The transformers in substation B. (c) The transformers in substation C. (d) The transformers in substation D. (e) The transformers in substation E. (f) The transformers in substation F.

by the traction calculation method and power flow calculation method [18]. With the train operating, the train position is changed. If the train stay on the stations, the train position is constant. When the train operates on traction condition, the traction current is positive. If the train operates on braking

condition, the traction current is negative. While, if the train operates on coasting condition or stays on stations, the traction current is 0. For example, at 2350 s, the train is operating from TPS #8 to TPS #9, located at 24.5 km, and the traction current is 0 A with coasting condition.

Assuming the headway is 200 s, and the dwell time is 40 s. The timetable of the DC metro line is shown in Fig. 10 of which each line expresses one single train. At any moment, obtaining the train positions in Fig. 10 and determining the train currents according to the train positions based on Fig. 9, the positions and values of the dc sources can be set in the proposed model. Thus, the dc current distribution in AC power system can be obtained. For example, at 800 s, there are 12 trains on the Shenzhen metro line. Seven trains operate on the up track and five trains operate on the down track. The train 1 shown as the green curve stays in the TPS #1 and prepares to operate from TPS #1 to TPS #14.

To obtain the dynamic result of the neutral dc current, multiple static simulations are completed with time step 1 s. Firstly, the train positions and traction current are sampled discretely with the time step of 1 s. Then, based on the static train positions and traction currents, the static simulation results are obtained any time steps [8]. Finally, arranging the static simulation results in chronological order, the neutral dc currents from 4000 s to 4800 s are obtained as shown in Fig. 10. When dc current flows into the transformers, the direction of the dc current is positive. If dc current flows out from the transformers, the direction of the dc current is negative.

### B. Distribution Characteristics of the DC Current

To obtain the dc current distribution characteristics, the differences of the neutral point dc currents of transformer in each substation are analyzed in detail.

The neutral point dc current of the substation A is shown in Fig. 11 (a). The maximin numbers are 30 A and -39 A. Obviously, the peak value of the neutral point dc current of substation A is larger than that of other substations. The reason may be mainly that the substation A is affected by the depot. In the depot, there is no SCCS and the rails are grounded directly. Thus, the current can flow into the grounding grid from the rails, which increases the stray current around the depot. Since the substation A is near the depot, the stray current can flow into the neutral grounded transformer in substation A largely.

The neutral point dc currents of the substation B and C are shown in Fig. 11 (b) and (c). The maximin numbers of the substation B are 12 A and -17 A. While the maximin numbers of the substation C are 7 A and -5 A. The substation B and C are both connected to the substation A as shown in Fig. 5. In time, the times of the maximum amplitudes of the neutral point dc current are very consistent, and the time interval is about 200s that is the headway time. In space, when the dc current of the substation A increasing, the dc currents of substation B and C mostly show the decrease. Moreover, the neutral point dc current of substation C is smaller than substation B and A because of the far distance between the substation and the DC metro line.

The neutral point dc currents of the substation D and E are shown in Fig. 11 (d) and (e). The two substations are both

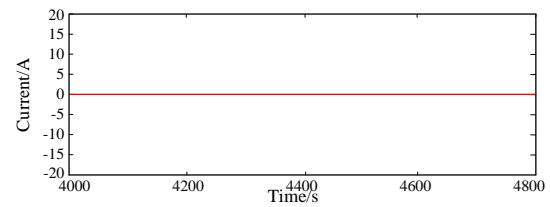


Fig. 12. The sum of the neutral dc current of substations A~F.

electrically connected to substation A. The maximin numbers of the substation D are 13.5 A and -15.2 A. While the maximin numbers of the substation E are 9.6 A and -8 A. Obviously, the neutral point dc current of substation D is larger than that of the substation E because of the substation E is farther away from the DC metro line. Moreover, when the dc current of the substation D decreasing, the dc current of substation E mostly shows the increase. The neutral point dc current of the substation F is shown in Fig. 11 (f). The maximin numbers are 10 A and -10.9 A. The substation E and F are electrically connected as shown in Fig. 5. When the dc current of substation E increases, the dc current of substation F mostly shows a decrease. Moreover, the times and the time interval of the maximum amplitudes of the substation D to F are the same with substations A to C.

The sum of the neutral dc current of substations A~F is shown in Fig. 12. The sum is always 0, which indicates that the sum of the dc currents flowing in the transformers is equal to the total dc currents flowing out the integral structure. In the proposed model, if the transformers A~F and the transmission lines among them are considered as an integral structure, the neutral points of the transformers are the ends of the integral structure. Moreover, the conductors of the integral structure are modeled only with dc resistances, and there is no dc current source in the AC power system. For this integral structure, the stray current of the Shenzhen metro line is the external dc current source of the integral structure. According to circuit principle, the sum of the currents flowing in the integral structure is equal to the total currents flowing out the integral structure. Thus the sum of neutral dc currents of the transformers is 0.

According to the analyses of the neutral point dc currents, there are some interesting distribution characteristics of the dc currents in the AC power system. In time, the direction of the neutral point dc current is changed with positive-negative alternating transformation. Moreover, the period time of the change approximately generally equals to the headway of the trains. In space, the magnitudes of neutral point dc currents of the transformers near the DC metro line especially the depot are larger than that of substations in the far away. Based on the distribution characteristics of the dc currents, the mitigation measures of dc bias should be taken at substations near the DC metro lines especially the depot and parking lot. Moreover, the positions of the new substations should be chosen away from the DC metro line, in particular away from the depot and parking lot.



## V. CONCLUSION

To evaluate the dc current distribution in AC power system caused by the stray current of DC metro system, a coupled simulation model is proposed. Through the analyses of the coupling relationship between the DC metro system and the AC power system, it shows the grounding system is an essential coupling element that should be considered in the proposed model. Based on the proposed model and the train operation conditions of the Shenzhen metro line, the dc current distribution in the AC power system is evaluated and analyzed in time and space. The analyses results show that the direction of the neutral point dc current is changed with positive-negative alternating transformation in time. Moreover, the period time of the change approximately equals to the headway of the trains. In space, the magnitude of neutral point dc currents of the transformers near the DC metro line especially the depot are larger than that of substations in the far away. Based on the distribution characteristics of the dc current, the mitigation measures of dc bias should be taken in the substations near the DC metro lines. In addition, the positions of the new substations should be chosen away from the DC metro line, in particular away from the depot and the parking lot.

## REFERENCES

- [1] Bo Zhang, Xiang Cui, Rong Zeng, and Jinliang He, "Calculation of dc current distribution in ac power system near hvdc system by using moment method coupled to circuit equations," *IEEE Transactions on Magnetics*, vol. 42, no. 4, pp. 703–706, April 2006.
- [2] F. Wu, S. Yu, Z. Zhao, and W. Quan, "Calculation and control of dc bias current distribution in an ac power system around a typical 800 kv dc grounding electrode," *The Journal of Engineering*, vol. 2019, no. 16, pp. 3145–3149, 2019.
- [3] L. L. Guang, S. X. Guo, and K. Wei, "Calculation of geomagnetically induced currents in interconnected north china-central china-east china power grid based on full-node gic model," *Power System Technology*, vol. 37, no. 7, pp. 1946–1952, 2014.
- [4] Z. Xie, X. Lin, Z. Zhang, Z. Li, W. Xiong, H. Hu, M. S. Khalid, and O. S. Adio, "Advanced dc bias suppression strategy based on finite dc blocking devices," *IEEE Transactions on Power Delivery*, vol. 32, no. 6, pp. 2500–2509, Dec 2017.
- [5] W. Li, Z. Pan, H. Lu, X. Chen, L. Zhang, and X. Wen, "Influence of deep earth resistivity on hvdc ground-return currents distribution," *IEEE Transactions on Power Delivery*, vol. 32, no. 4, pp. 1844–1851, Aug 2017.
- [6] C. A. Charalambous, I. Cotton, P. Aylott, and N. D. Kokkinos, "A holistic stray current assessment of bored tunnel sections of dc transit systems," *IEEE Transactions on Power Delivery*, vol. 28, no. 2, pp. 1048–1056, April 2013.
- [7] A. Ogunsola, A. Mariscotti, and L. Sandrolini, "Estimation of stray current from a dc-electrified railway and impressed potential on a buried pipe," *IEEE Transactions on Power Delivery*, vol. 27, no. 4, pp. 2238–2246, Oct 2012.
- [8] C. A. Charalambous and P. Aylott, "Dynamic stray current evaluations on cut-and-cover sections of dc metro systems," *IEEE Transactions on Vehicular Technology*, vol. 63, no. 8, pp. 3530–3538, Oct 2014.
- [9] A. Ogunsola, L. Sandrolini, and A. Mariscotti, "Evaluation of stray current from a dc-electrified railway with integrated electric-electromechanical modeling and traffic simulation," *IEEE Transactions on Industry Applications*, vol. 51, no. 6, pp. 5431–5441, Nov 2015.
- [10] S. Y. Xu, W. Li, and Y. Wang, "Effects of vehicle running mode on rail potential and stray current in dc mass transit systems," *IEEE Transactions on Vehicular Technology*, vol. 62, no. 8, pp. 3569–3580, Oct 2013.
- [11] S. Yang, G. Zhou, and Z. Wei, "Influence of high voltage dc transmission on measuring accuracy of current transformers," *IEEE Access*, vol. 6, pp. 72 629–72 634, 2018.
- [12] Z. Pan, L. Zhang, X. Wang, H. Yao, L. Zhu, Y. Liu, and X. Wen, "Hvdc ground return current modeling in ac systems considering mutual resistances," *IEEE Transactions on Power Delivery*, vol. 31, no. 1, pp. 165–173, Feb 2016.
- [13] Y. Zhao, P. A. Crossley, and T. David, "Impact of dc bias on operating performance of current transformers," *The Journal of Engineering*, vol. 2018, no. 15, pp. 930–934, 2018.
- [14] F. P. Dawalibi, Y. Li, C. Li, and J. Liu, "Mitigation of transformer saturation due to neutral hvdc currents," in *2005 IEEE/PES Transmission Distribution Conference Exposition: Asia and Pacific*, Aug 2005, pp. 1–6.
- [15] N. Yan-Ru, Z. Xiang-Jun, Y. Kun, L. Yang, and P. Ping, "Research on modeling method of transformer dc bias caused by metro stray current," in *2018 International Conference on Power System Technology (POWERCON)*, Nov 2018, pp. 3834–3839.
- [16] C.-H. Lee and C.-J. Lu, "Assessment of grounding schemes on rail potential and stray currents in a dc transit system," *IEEE Transactions on Power Delivery*, vol. 21, no. 4, pp. 1941–1947, Oct 2006.
- [17] S.-L. Chen, S. Hsu, C.-T. Tseng, K.-H. Yan, H.-Y. Chou, and T.-M. Too, "Analysis of rail potential and stray current for taipei metro," *IEEE Transactions on Vehicular Technology*, vol. 55, no. 1, pp. 67–75, Jan 2006.
- [18] Y. V. Bochamnikov, A. M. Tobias, C. Roberts, S. Hillmanssen, and C. J. Goodman, "Optimal driving strategy for traction energy saving on dc suburban railways," *IET Electric Power Applications*, vol. 1, no. 5, pp. 675–682, Sept 2007.
- [19] GB 50157-2013 Code for design of metro, Ministry of Housing and Urban-Rural Development of the People's Republic of China (MOHURD).
- [20] GB 50065-2011 Code for design of ac electrical installations earthing, Ministry of Housing and Urban-Rural Development of the People's Republic of China (MOHURD).
- [21] IEEE Guide for Safety in AC Substation Grounding, IEEE Std. 80-2000, pp. 1-199.
- [22] *CDEGS Software, Safe Eng. Services Technol. Ltd., Montral, QC, Canada*, 1978.
- [23] Y. Tzeng and C. Lee, "Analysis of rail potential and stray currents in a direct-current transit system," *IEEE Transactions on Power Delivery*, vol. 25, no. 3, pp. 1516–1525, July 2010.
- [24] GB/T 28026.2-2018 Railway applications, Fixed installations, Part 2: protective provisions against the effects of stray current caused by dc traction supply system.
- [25] Railway applications, Fixed installations, Part 2: protective provisions against the effects of stray current caused by dc traction supply system, EN 50122-2, Oct. 2012.
- [26] Railway applications, Fixed installations, Part 2: protective provisions against the effects of stray current caused by dc traction supply system, IEC 62128-2, Sept. 2013.
- [27] "Hvdc ground electrode design," IEC, San Francisco, CA. 1981. EPRI EL-2020, Project 1467-1.
- [28] L. G. Liu, X. Y. Zhao, M. S. Zhang, Y. Q. Yan, and P. Zhu, "Influence of dc bias suppression of grounding electrodes on power grid gic," *Power System Technology*, vol. 42, no. 11, pp. 3594–3600, 2018.
- [29] R. Horton, D. Boteler, T. J. Overbye, R. Pirjola, and R. C. Dugan, "A test case for the calculation of geomagnetically induced currents," *IEEE Transactions on Power Delivery*, vol. 27, no. 4, pp. 2368–2373, Oct 2012.



**Aimin Wang** received the B.S. and M.S. degrees in Control Theory and Control Engineering from Changan University, Xian, China, in 2014 and 2017, respectively. She is currently working toward the Ph.D. degree in the School of Electrical Engineering, Southwest Jiaotong University, Chengdu, China.

Her research interest includes analysis and control of Metro Stray Current.



**Sheng lin** received the B.Sc. and Ph.D. degrees from Southwest Jiaotong University, Chengdu, China, in 2006 and 2011, respectively. From 2009 to 2010, he was a Visiting Scholar with North Carolina State University, Raleigh, NC, USA. He is currently a professor in School of Electrical Engineering in Southwest Jiaotong University, Chengdu, China.

His research interests include analysis and control of Metro Stray Current, prediction and health management of Traction Power Supply System, protection and control of AC/DC Hybrid System.



**Ziheng Hu** received the B.E., M.E. and Ph.D. degree from Southeast University, Nanjing, China, in 1985, 1988 and 1992, respectively. He is currently a deputy general manager in Shenzhen Power Supply Bureau. His research interests include technical management of power grid operation and control.



**Junyi Li** received the B.S. degrees in Electrical Engineering and Automation from Hangzhou Dianzi University, Hangzhou, China, in 2018. He is currently working toward the M.S. degree in the School of Electrical Engineering, Southwest Jiaotong University, Chengdu, China. His research interest includes analysis and control of Metro Stray Current.



**Feng Wang** received B.Sc degrees from Shijiazhuang Tiedao University, Shijiazhuang, China, in 2013. He is currently a master in School of Electrical Engineering in Southwest Jiaotong University, Chengdu, China. His research interest is analysis and control of Metro Stray Current.



**Guoxing Wu** received the B.E. and M.E. degree from North China Electric Power University, Beijing, China, in 2002 and 2005, respectively. He is currently a department director in Shenzhen Power Supply Bureau. His research interests include transformer DC bias, high voltage and insulation technology.



**Zhengyou He** received the B.Sc. and M.Sc. degrees in Computational Mechanics, in Chongqing University, Chongqing, China, in 1992 and 1995, respectively, and the Ph.D. degree in Electrical Engineering in Southwest Jiaotong University, Chengdu, China, in 2001. Currently, he is a professor in School of Electrical Engineering in Southwest Jiaotong University, Chengdu, China. His research interests include signal processing, fault diagnosis and reliability analysis in Power Systems and High-speed Railway Traction Power

Supply System.